1-1-2019

Triassic turbidites in the West Qinling Mountains, NW China: Part of the collisional Songpan-Ganzi Basin or an active forearc basin?

Zhen Yan
Chinese Academy of Geological Sciences

Changlei Fu
Chinese Academy of Geological Sciences

Jonathan C. Aitchison
University of Queensland, jonathan.aitchison@sydney.edu.au

Solomon Buckman
University of Wollongong, solomon@uow.edu.au

Manlan Niu
Hefei University of Technology

See next page for additional authors

Triassic turbidites in the West Qinling Mountains, NW China: Part of the collisional Songpan-Ganzi Basin or an active forearc basin?

Abstract

Lower to Middle Triassic clastic rocks in the West Qinling Mountains along NE margin of the Qinghai-Tibet Plateau are generally regarded as part of the Songpan-Ganzi flysch Basin. However relatively little attention has been paid to the age and provenance of these units. New petrological and geochemical results demonstrate that these sediments accumulated along an active continental margin and are dominated by feldspathic litharenite and lithic arkose with low mineral and compositional maturity. They were derived primarily from a continental arc source dominated by intermediate to felsic igneous rocks, with a minor contribution from older metamorphosed and sedimentary sources. Turbidite samples yielded two primary detrital zircon U-Pb age populations of ca. 273 Ma and ca. 435 Ma, which is different from the Early Triassic (ca. 252 Ma) and Middle Silurian (ca. 427 Ma) age populations that dominate the Songpan-Ganzi Basin. These data together with paleocurrent results indicate that the South Qilian Belt was the primary source origin because this belt contains both early Paleozoic Andean-type igneous and magmatic rocks and has a basement of Precambrian metamorphosed rocks. Regionally, an Andean-type arc traverses the South Qilian belts and extends into the West Qinling Mountains and Kunlun Orogen, which formed by north-directed subduction of the Paleo-Tethyan Ocean during the Early to Middle Triassic. Voluminous detritus that originated from the Qilian and Kunlun orogens as they were uplifted and eroded was transported to the south and deposited in the forearc area in front of the A'nimaqen-Mianlue suture.

Publication Details

Yan, Z., Fu, C., Aitchison, J. C., Buckman, S., Niu, M. & Cao, B. (2019). Triassic turbidites in the West Qinling Mountains, NW China: Part of the collisional Songpan-Ganzi Basin or an active forearc basin?. Journal of Asian Earth Sciences: X, 100020-1-100020-13.

Authors

Zhen Yan, Changlei Fu, Jonathan C. Aitchison, Solomon Buckman, Manlan Niu, and Bo Cao

Journal of Asian Earth Sciences: X xxx (xxxx) xxxx

Contents lists available at ScienceDirect

Journal of Asian Earth Sciences: X

journal homepage: www.journals.elsevier.com/journal-of-asian-earth-sciences-x

Triassic turbidites in the West Qinling Mountains, NW China: Part of the collisional Songpan-Ganzi Basin or an active forearc basin?

Zhen Yan[a,*], Changlei Fu[a], Jonathan C. Aitchison[b], Solomon Buckman[c], Manlan Niu[d], Bo Cao[a]

[a] Institute of Geology, Chinese Academy of Geological Science, Beijing 100037, China
[b] School of Earth and Environmental Sciences, University of Queensland, Brisbane, St Lucia, Qld 4072, Australia
[c] School of Earth and Environmental Sciences, University of Wollongong, Wollongong, NSW 2522, Australia
[d] Department of Resources and Environment, Hefei University of Technology, Hefei 230009, China

ARTICLE INFO

Keywords:
Geochemistry
Provenance
Forearc basin
Andean-type continental margin
West Qinling Mountains

ABSTRACT

Lower to Middle Triassic clastic rocks in the West Qinling Mountains along NE margin of the Qinghai-Tibet Plateau are generally regarded as part of the Songpan-Ganzi flysch Basin. However relatively little attention has been paid to the age and provenance of these units. New petrological and geochemical results demonstrate that these sediments accumulated along an active continental margin and are dominated by feldspathic litharenite and lithic arkose with low mineral and compositional maturity. They were derived primarily from a continental arc source dominated by intermediate to felsic igneous rocks, with a minor contribution from older metamorphosed and sedimentary sources. Turbidite samples yielded two primary detrital zircon U-Pb age populations of ca. 273 Ma and ca. 435 Ma, which is different from the Early Triassic (ca. 252 Ma) and Middle Silurian (ca. 427 Ma) age populations that dominate the Songpan-Ganzi Basin. These data together with paleocurrent results indicate that the South Qilian Belt was the primary source origin because this belt contains both early Paleozoic Andean-type igneous and magmatic rocks and has a basement of Precambrian metamorphosed rocks. Regionally, an Andean-type arc traverses the South Qilian belts and extends into the West Qinling Mountains and Kunlun Orogen, which formed by north-directed subduction of the Paleo-Tethyan Ocean during the Early to Middle Triassic. Voluminous detritus that originated from the Qilian and Kunlun orogens as they were uplifted and eroded was transported to the south and deposited in the forearc area in front of the A'nimaqen-Mianlue suture.

1. Introduction

Clastic sediments are composed of different minerals and detritus derived from pre-existing source rocks. Their compositions are closely related to provenance and the tectonic settings of sedimentary basins. Studies of the provenance of siliciclastic rocks can provide robust information for understanding basin development by linking sediment supply to exhumation episodes and tectonic evolution (e.g., Japsen et al., 2007; Weislogel et al., 2006, 2010; Sun et al., 2016; Higgs and King, 2018) and allows the reconstruction of sediment transport routes (e.g., Dickinson and Gehrels, 2009; Olivarius et al., 2014; Yan et al., 2014; Pe-Piper et al., 2016). Diverse techniques based on petrographical and geochemical criteria have been successfully used in ancient rocks for this purpose (e.g., She et al., 2006; Ryan and Williams, 2007; Dickinson and Gehrels, 2008; Yan et al., 2008, 2012, 2014; Sun et al., 2016). In addition, chemically immobile elements in siliciclastic rocks such as rare earth elements (REE) and some trace elements of Th, Zr, Hf, and Sc also provide information on the degrees and types of weathering, which is useful in developing an understanding of the regional setting of basin development.

Triassic flysch in the West Qinling Mountains is traditionally regarded as a component of the collisional Songpan-Ganzi Basin in the NE Tibetan Plateau (Nie et al., 1994; Zhou and Graham, 1996; Brugier et al., 1997; Enkelmann et al., 2007; Weislogel et al., 2010). These turbidite deposits have commonly been interpreted as the erosional products associated with uplift during closure of the Paleo-Tethyan Ocean basin between the North China-Tarim plate and Qaidam block to the north, the South China plate to the east, and the Qiangtang terrane and Yidun arc terrane to the south (Sengör et al., 1988; Stampfli and Borel, 2002; Weislogel, 2008; Li et al., 2017, 2018; Fig. 1a). Although these sediments have been studied before, most work focuses on interpretation of detrital zircons in sandstones from the southern Songpan-Ganzi Basin and less attention has been paid in the West Qinling Mountains. There is still no agreement on the provenance and

* Corresponding author.
E-mail address: yanzhen@mail.igcas.ac.cn (Z. Yan).

https://doi.org/10.1016/j.jaesx.2019.100020
Received 17 May 2019; Received in revised form 22 September 2019; Accepted 29 September 2019

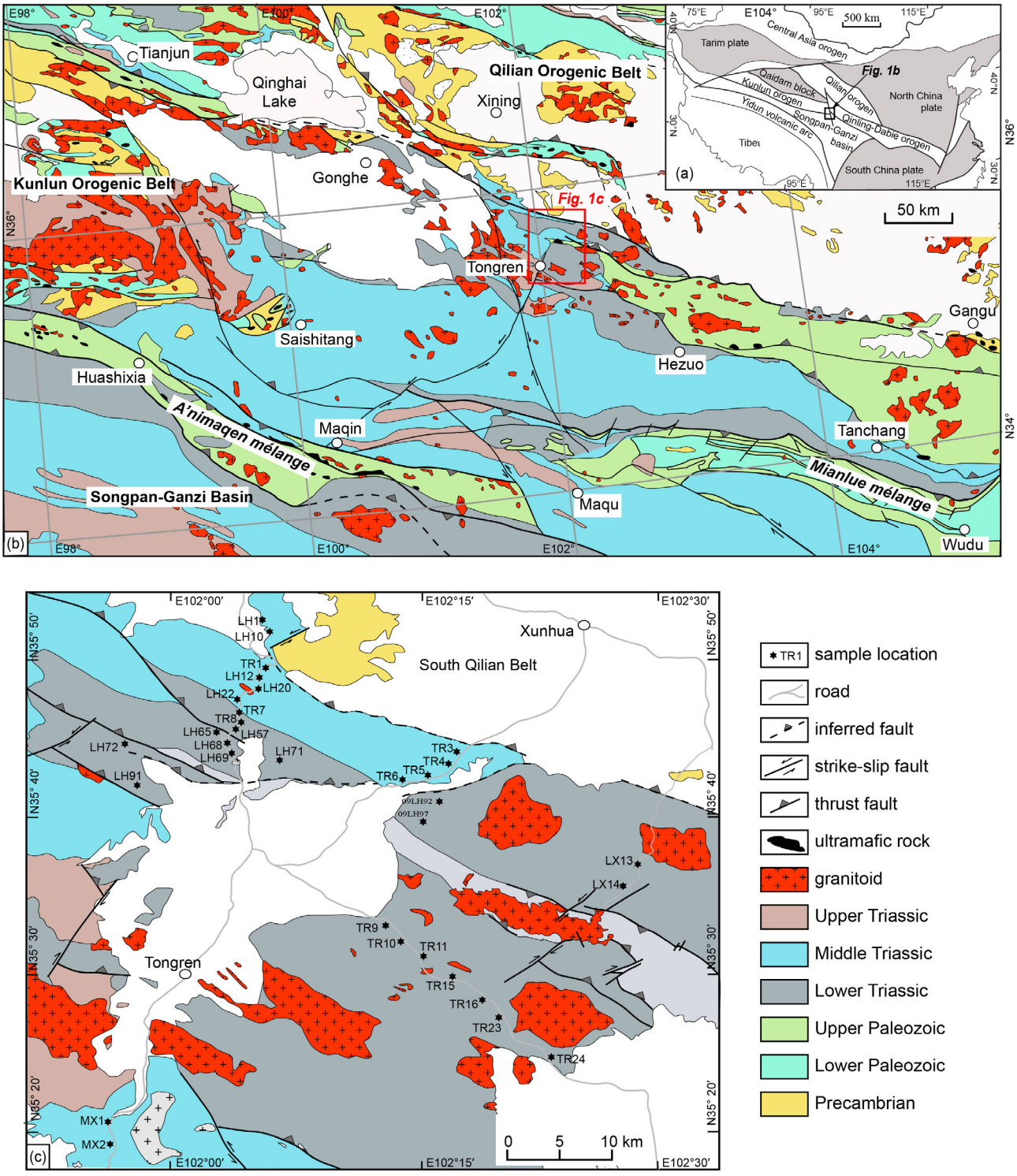

Fig. 1. (a) Tectonic framework of the Chinese Central Orogenic Belt that comprises the Qilian, Kunlun and Qinling orogens and the location of the West Qinling Mountains. (b) Regional geological map of the West Qinling Mountains showing the relationship between the Qilian and Kunlun orogens and Songpan-Ganzi basin and location of study area. (c) Detailed geological map of the study area and locations of the studied samples.

depositional setting of the Songpan-Ganzi Basin. In contrast, a distinct synthesis based on petrology and geochemistry of ophiolite and the associated rocks in the West Qinling Mountains and Kunlun Orogen (Xu et al., 1996; Xiao et al., 2002; Bian et al., 2004; Guo et al., 2012; X.W. Li et al., 2013, 2014) infers that a Triassic Andean-type continental margin (Yan et al., 2012, 2014) developed in response to the northward subduction of the Paleo-Tethyan Ocean. However, Li et al. (2017, 2018) suggested that all the continental blocks in China were assembled to form the Supercontinent Pangea around ~250 Ma, indicating that the Paleo-Tethyan Ocean closed prior to 250 Ma and the Lower to Middle Triassic sediments in the Songpan-Ganzi Basin were not related to subduction of the Paleo-Tethyan Ocean.

In order to address this controversy, we assess the provenance of Triassic flysch in the West Qinling Mountains focusing on the geochemistry of fine-grained siliciclastic rocks and two detrital zircon U-Pb dating samples. Using these new data in combination with regional

geology and previous published data, we discuss the tectonic setting in which deposition occurred and the associated evolution of the Paleo-Tethyan Ocean in the West Qinling Mountains between the North and South China plates.

2. Geological setting

The West Qinling Mountains is a geologically significant portion of the Qinling Orogenic Belt. This belt extends for more than 1000 km across eastern Asia and separates the North China Plate to the north from the South China Plate to the south. To the north and west, the West Qinling Mountains connect with the Qilian and Kunlun orogenic belts (Fig. 1b), respectively. To the south, they are separated from the Songpan-Ganzi Basin by a latest middle-Triassic ophiolitic mélange along the A'nimaqen-Mianlue fault.

The A'nimaqen-Mianlue mélange consists of Cambrian-Ordovician and Carboniferous-Early Permian ophiolitic blocks within a matrix of Lower to Middle Triassic flysch (Xu et al. 1996; Bian et al. 2004; Yang et al. 2004; Guo et al. 2007) and represents the northeasternmost branch of the Paleo-Tethyan Ocean (Meng and Zhang, 1999; Lai et al., 2004). Another zone of mélange occurs along the Qinghai Lake Fault on the northern margin of the West Qinling Mountains (Wang et al., 2000; Guo et al., 2007). Assemblages of Devonian-Permian mafic-ultramafic rocks, pillow basalt, gabbro, and radiolarian chert, together with Proterozoic metavolcanic blocks, are tectonically intermingled with Carboniferous-Permian arc-related volcanic rocks in the Saishitang area (Wang et al. 2000; Sun et al. 2004). Geochemical investigations by Wang et al. (2000) and Guo et al. (2007) demonstrate that pillow basalts in this area originated in a backarc basin setting related to northward subduction of the Paleo-Tethyan Ocean (Yang et al., 2004). These mélanges are intruded by Early- to Middle-Triassic arc granites (Xiao et al., 2002; Guo et al., 2012; Yan et al., 2012; Xie et al., 2015). In addition, andesite, dacite, and rhyolite interlayers are common among the Middle Triassic sediments, and the Late Triassic rock record is dominated by andesites and associated pyroclastic rocks. These observations indicate Middle to Late Triassic arc magmatism in the West Qinling Mountains. Together the relative ages of ophiolitic mélanges and accreted arc-related volcanic and granitoid rocks appear to progressively young southward across the West Qinling Mountains, implying southward trench migration during evolution of the Paleo-Tethyan Ocean (Yan et al., 2012).

Triassic sedimentary-volcanic assemblages in the West Qinling Mountains are subdivided into three regional scale mappable units (BGMRGP, 1989; BGMRQP, 1991). The Lower Triassic Longwuhe Group consists of locally fossiliferous deep marine turbidite sediments typical of a submarine fan depositional setting. The Middle Triassic Gulangdi Formation represents a large-scale sedimentary succession shallowing upward from proximal continental slope turbidites through to fluviodeltaic sediments in higher parts of the section (Fig. 2; Yan et al., 2012, 2014). The Elashan Group is mainly exposed in the west of the Saishitang area and consists of andesite, dacite, rhyolite, and pyroclastic rocks, showing typical Andean-style petrological characteristics. Our recent SHRIMP zircon U-Pb dating and geochemical data demonstrate that this assemblage of andesite, dacite, and volcaniclastic rocks formed in an arc setting during the Middle Triassic around 240.1 ± 2.4 Ma. Together these rocks represent the products of convergent continental margin slope sedimentation and volcanism from Early to Middle Triassic time.

Regionally, the Longwuhe Group and Gulangdi Formation nonconformably overlie the ophiolite complex in the West Qinling Mountains. They have been correlated with the Liufengguan Group in the Qinling Orogen to the east and the Hongshuichuan and Naocangjian formations in the Kunlun Orogen to the west (BGMRGP, 1989; BGMRQP, 1991). These strata are commonly considered to be a northern portion of the famous Songpan-Ganzi Basin, but few detailed studies exist regarding the age and provenance of this basin. Several distinct end-member hypotheses suggest that the Songpan-Ganzi Basin represented a remnant ocean basin (Zhou and Graham, 1996; Enkelmann et al., 2007; Weislogel, 2008; Weislogel et al., 2010), a rift basin (Chen et al., 1987; Chang, 2000), a non-extensional back-arc basin (Klimetz, 1983; Gu, 1994; Tang et al., 2018), or a Mediterranean-style back-arc basin that opened in association with oceanic slab rollback (Pullen et al., 2008; Ding et al., 2013; L. Li et al., 2014; X.W. Li et al., 2014). These interpretations are mainly based on detrital zircon U-Pb ages or limited geochemistry of sandstones from the southern portion of this basin. However, a collision-related strike-slip pull-apart basin (Feng et al. 2002; Sun et al. 2004) or foreland basin (Kou et al. 2007) origin has been suggested to Triassic sediments in the West Qinling Mountains, implying that the Paleo-Tethyan Ocean closed prior to the Early Triassic. In contrast, other studies suggested that the Triassic sediments in the West Qinling Mountains were deposited in a forearc basin that formed in association with northward subduction of the Paleo-Tethyan Ocean along the A'nimaq-Mianlue suture (Jiang et al., 1996; Yan et al., 2008, 2012, 2014; Guo et al., 2012; Li et al., 2015).

3. Sampling and analytical methods

In order to further define the composition of Lower- and Middle-Triassic sediments and their potential source rocks, thin-sections of fine- and coarse-grained sandstone and mudstone samples were observed under a polarizing microscope. A total of 32 representative samples including 18 mudstones, 11 siltstones, and three lithic arkoses from around Tongren area (Fig. 1c) were selected for geochemical analysis, and two medium-grained arkose samples (LW1 and TR7) were collected for detrital zircon U-Pb dating. Samples were ground in an agate mill and zircon separation was undertaken at the Laboratory of the Institute of Regional Geology and Mineral Survey Research of Hebei Province.

The analytical procedures used were X-Ray fluorescence (XRF) spectrometer for major element analysis and inductively coupled plasma mass spectrometry (ICP-MS) for trace elements. All analyses were performed at National Research Center for Geoanalysis, Beijing, following standard procedures for each method. International standards GSR1, GSR2, and GSR3 were used to monitor analytical quality control. Detection limits for major elements were < 0.01% (except for TiO_2 and MnO, which had detection limits < 0.001%). Detection limits for trace elements were 1–0.05 ppm. Based on the analyses of international reference materials, the analytical precision for all major oxides by XRF is estimated to be better than 1% and the analytical error ranges for trace elements are within 5–10%. Appendix 1 contains the results of geochemical analyses for all samples.

Zircon grains from sandstones were extracted using standard heavy liquid and magnetic techniques. They were handpicked under a binocular microscope, and mounted in epoxy resin. The sample mount was polished to expose the center of the zircon grains and then gold-coated. Cathodoluminescence (CL) images were acquired to reveal internal structures using scanning electron microscopy, and U-Th-Pb zircon dating was performed on the laser-ablation-inductively coupled plasma-mass spectrometry (LA-ICP-MS) at the Beijing Createch Testing Technology Co., Ltd. Zircon GJ1 was used as external standard for U-Pb dating, and was analyzed twice every 10 analyses. Preferred U-Th-Pb isotopic ratios used for GJ1 are from Jackson et al. (2004). In the presentation of figures, tables, and results we follow Gehrels et al. (2006) with $^{206}Pb/^{238}U$ ages quoted for zircons younger than 1.0 Ga, and older grains are quoted using their $^{207}Pb/^{206}Pb$ ages. Discordant data were excluded from the relative probability calculation. Zircon analyses with < 10% normal discordance are considered to be geologically meaningful (Dickinson and Gehrels, 2008) and are used to date the maximum age of deposition. The age calculations and concordia diagrams were made using Isoplot/Ex ver. 3.0 (Ludwig, 2003). The U-Pb data are listed in Appendix 2.

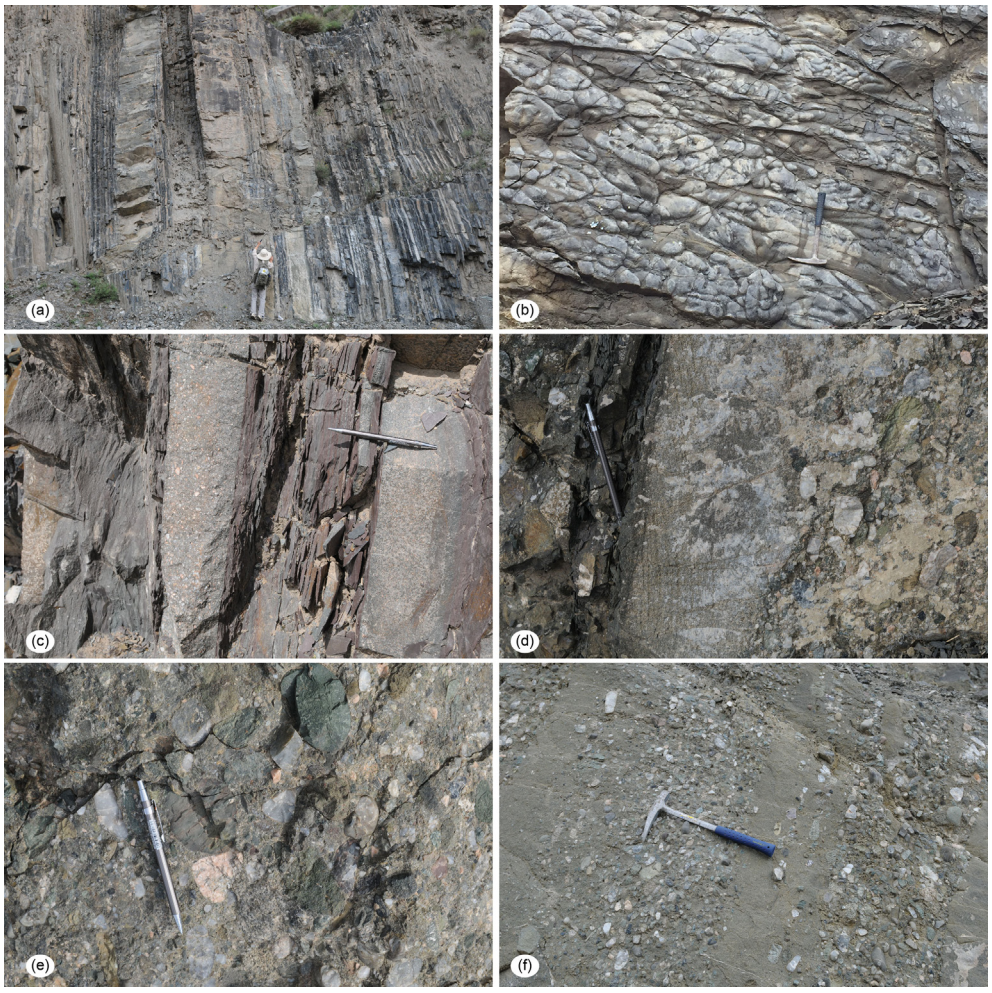

Fig. 2. Field photographs showing the characteristics of Triassic sediments in the West Qinling Mountains. Longwuhe Group: (a) Turbiditic rhythms of sandstone, siltstone, and black mudstone with a variable thickness of 3–75 cm. Geologist in the middle as scale. (b) Flute-marks on turbidite siltstone surface indicating paleocurrent to the SW. Hammer is 40 cm long. Gulangdi Formation: (c) Turbiditic siltstone and mudstone rhythms with lenticular conglomerate showing normal grading and ripple lamination. Pen is 14 cm long and the nib points to the top (left). (d) Lens of conglomerate and sandstone with planar cross-bedding and erosional surface at irregular base (right), indicating channel deposits. Pen is 14 cm long and the nib points to SW direction of paleocurrent (lower right side). (e) Sand-supported conglomerate containing rounded basalt, quartzite, granite, and minor marble clasts. (f) Fluvial deposits of conglomerate and sandstone showing imbricated clasts and crude cross-bedding.

4. Sandstone petrology

Sandstones in the Longwuhe Group are dominated by lithic arkose and litharenite containing abundant volcanic and metamorphic fragments. Those from the Gulangdi Formation consist mainly of feldspathic litharenite and lithic arkose, characterized by abundant feldspar, volcanic, and granitic fragments with minor carbonate and metamorphic fragments (Fig. 3). Siltstone contains abundant fine-grained feldspar and minor quartz and volcanic fragments, and mudstone is dominated by detrital sericite with minor fine-grained feldspar and quartz grains. Detrital heavy mineral analyses by Yan et al. (2014) demonstrate that sandstones commonly contain zircon, rutile, garnet, tourmaline, and epidote grains. Minor amphibole, pyroxene, and Cr-spinel grains occur in some sandstone samples.

Overall, the composition of sandstones mainly consists of volcanic (average 26%), granitoid (average 38%), and metamorphic (average 28%) fragments, with minor (8–20%) sedimentary fragments including chert, silty mudstone, and limestone (Yan et al., 2014), indicating a continental arc source. Feldspar grains are dominated by plagioclase. Rare mica and epidote grains were observed within litharenite and lithic arkose. Abundance of quartz clasts varies from 5% to 17% of framework grains, which is low in comparison to those of other grains. Most quartz grains are polycrystalline with obvious scaly inclusions and undulose extinction indicating metamorphic origins, whereas monocrystalline quartz commonly contains fluid inclusions and likely originated from plutonic rocks (Basu et al., 1975). Clear, fluid inclusion-free quartz with uniform extinction and embayment textures, interpreted to be volcanic in origin, is also common.

5. Results

5.1. Geochemistry

The analyzed samples have a similar average major element geochemistry, indicating a similar mineralogy. Four siltstone samples from the Longwuhe Group exhibit lower SiO_2 (43.34–49.59%) and Al_2O_3 (12.86–14.39%) abundance and higher abundance of CaO (7.09–17.72%) and loss on ignition (LOI; 7.21–14.59%), indicating the presence of detrital grains with carbonate and/or calcareous cement. Other samples have a variable and higher range of SiO_2 content (51.93–61.16%) and exhibit variable negative correlation with Al_2O_3, K_2O, MgO, FeO^T, MnO and P_2O_5 (Fig. 4), reflecting the quartz dilution effect. Al_2O_3 shows positive correlation with K_2O, MgO, FeO^T and TiO_2, but the mean K_2O/Al_2O_3 ratio for all samples is < 0.2. Compared with upper continental crust compositions (UCC), all samples are slightly enriched in TiO_2, Al_2O_3, FeO^T, MgO, and P_2O_5 and distinctly depleted in NaO_2 and SiO_2, indicating a low maturity.

Samples from the Longwuhe Group show variable and relatively low Cs, Ba, Rb, Sr, and Cr than contents compared to the Gulangdi Formation, but their mean contents are similar to UCC. No distinct correlation is observed between Al_2O_3 and Sc, Cr and V, suggesting that these trace element contents are not controlled by clay minerals. The total REE (ΣREE) contents of the Longwuhe Group samples are the most varied, ranging from 65 to 226 ppm (avg. 165 ppm), which is lower than that of the Gulangdi Formation samples (ΣREE = 116–359 ppm; avg. 198 ppm). Chondrite-normalized REE patterns (Fig. 5) are enriched in light REE (LREE), corresponding to variable LREE/HREE

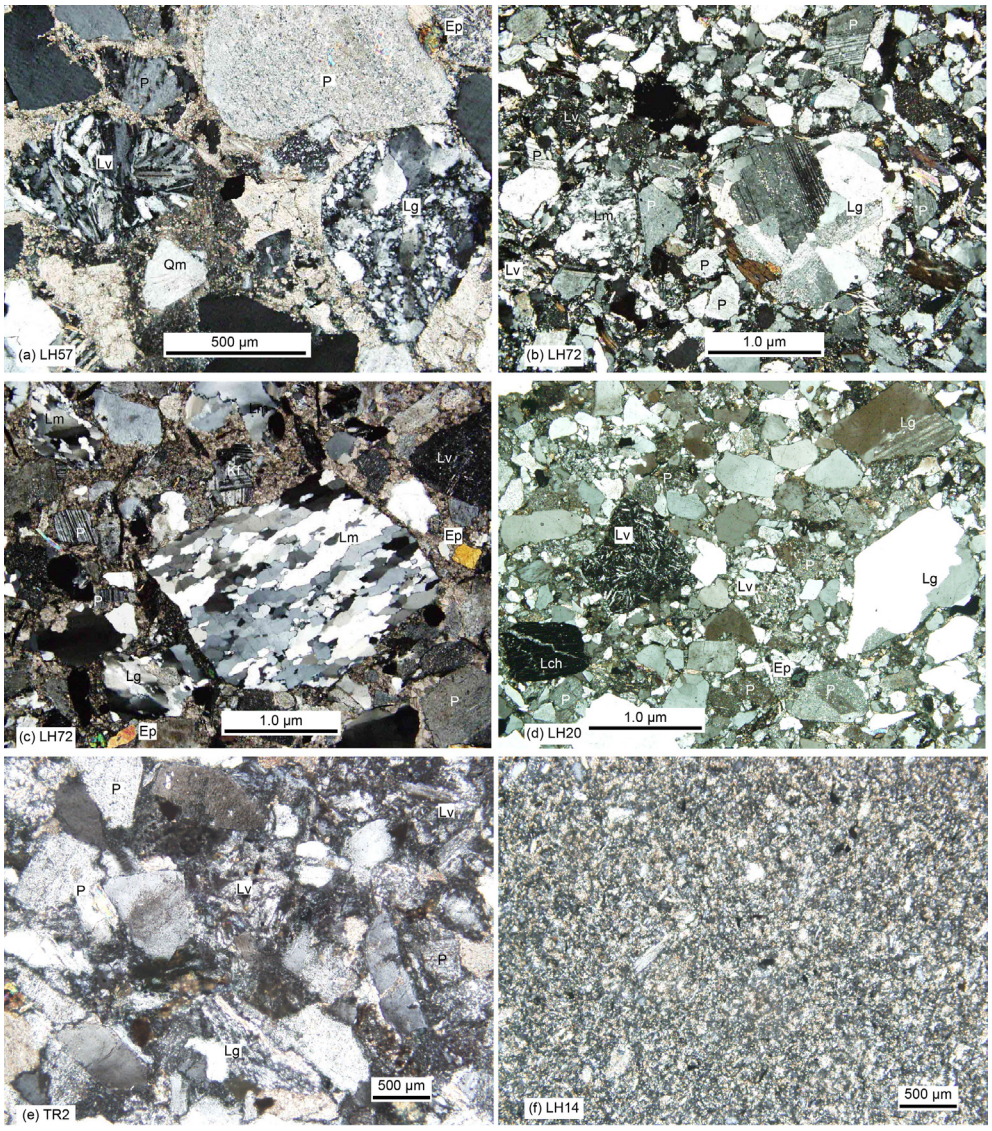

Fig. 3. Photomicrographs of sandstone samples. Longwuhe Group: (a) coarse-grained lithic arkose containing subrounded volcanic (Lv), granitic (Lg), plagioclase (P), and minor quartz detritus. Monocrystalline quartz grains (Qm) commonly contain fluid inclusions. (b) and (c) Litharenite containing angular to subangular granitic (Lg), metamorphic (Lm), volcanic (Lv), plagioclase (P), and minor k-feldspar (Kf) and epidote (Ep) grains. Metamorphic fragment (Lm) consisting of oriented quartz. Gulangdi Formation: (d) Coarse-grained feldspathic litharenite containing abundant granitic (Lg), volcanic (Lv), chert (Lch), and plagioclase (P) fragments. (e) Medium-grained lithic arkose consisting of plagioclase (P), volcanic (Lv), granitic (Lg) fragments and minor quartz grains. (f) Siltstone consisting of fine-grained feldspar and quartz.

enrichments (La_N/Yb_N = 2.68–12.42). The average Eu anomaly (Eu/Eu*) is 0.32 (range between 0.06 and 0.84), which is less depleted in Eu than UCC (0.72; Rudnick and Gao, 2003). ΣREE values show a weak positive correlation with Al_2O_3, P_2O_5 and TiO_2, and the total heavy REE (HREE) contents show strong positive correlation with Y (r = 0.99). These observations demonstrate the differing amounts and variable influence of minerals including allanite, monazite, apatite, and zircon in the control of REE contents of these rocks (McLennan et al., 1993).

5.2. U-Pb data

Sample LW1 This sample was collected from the Gulangdi Formation and contained limited zircon grains. Zircons are elongate and rounded grains with a long axial of 50–100 μm, showing faintly banded or concentric oscillatory zoning in CL image. Some have a thinner and irregular overgrowth with bright luminescence. Forty spots on the 40 dated grains yielded a concordant $^{206}Pb/^{238}U$ age of 270–2547 Ma (Fig. 6a), with a dominant peak at 440 Ma (n = 21) and a subordinate peak at 277 Ma (n = 6). Several minor peaks include 658, 920, 1122–1250, 1385, and 2544 Ma. These spots have a wide range of U contents (19–1009 ppm) and variable but high Th/U ratios of 0.11–3.61 (avg. 0.98).

Sample TR7 This sample was collected from the Longwuhe Group and contained abundant rounded and equant zircon grains. Most have a concentric or faintly banded or sector zoning, and others have a well-developed core-rim texture consisting of a small core with irregular boundary and a wide rim with banded zoning. Five-nine of the 61 dated zircon grains yielded concordant $^{206}Pb/^{238}U$ age of 232–2493 Ma (Fig. 6b), with a dominant peak at 447 Ma (n = 13) and a subordinate peak at 1837 Ma (n = 10). The other grains yielded several minor age peaks at 256, 312, 863, 1583, 1767, 1978, 2331, 2409 and 2480 Ma. Analyzed spots have variable U contents of 18–615 ppm and Th/U ratios between 0.01 and 2.04 (avg. 0.56).

6. Paleoweathering conditions and recycling

6.1. Paleoweathering conditions

Provenance and the intensity of weathering in the source region are the main factors that control the chemical and mineralogical composition of siliciclastic rocks. Generally, large ionic radius cations such as Cs, Rb and Ba are relative immobile during chemical weathering processes and preferentially fixed in weathering profiles by adsorption clays, while smaller cations like Na, Ca and Sr are selectively leached from them (McLennan et al., 1993). Therefore, the effects of alteration have to be seriously considered before the composition of sediments can be used to assess source composition and tectonic setting.

The Chemical Index of Alteration (CIA; Nesbitt and Young, 1982) or

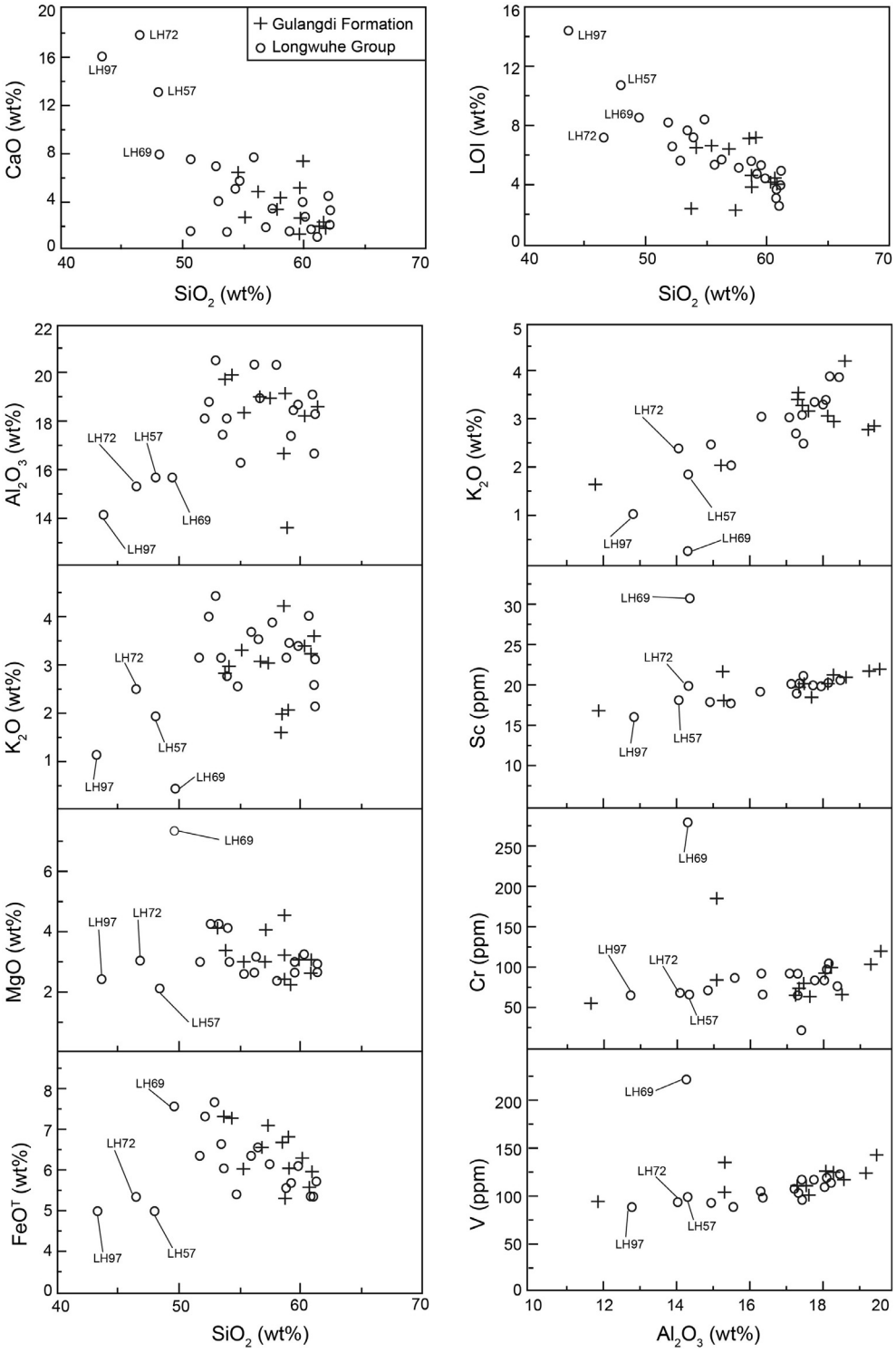

Fig. 4. Variations of SiO_2 versus major oxides (wt%) and LOI (wt%) and Al_2O_3 versus K_2O (wt%), and Sc, Cr and V (ppm) for siliciclastic rocks.

the Chemical Index of Weathering (CIW; Harnois, 1988) is a useful tool with which to evaluate the degree of source area weathering and quantify the amount of chemically weathered materials included in siliciclastic sediments. Variations also reflect changes in mineralogical composition. Generally, CIA values vary from 60 or less for slightly weathered igneous rocks to near 100 for residual clays enriched in kaolinite and/or gibbsite. The samples exhibit a variable CIA value ranging from 51 to 71 with average of 64, which is higher than fresh basalts (30–45) and granites (45–55; Nesbitt and Young, 1982) and unweathered UCC (48; Rudnick and Gao, 2003) but less than PAAS and cratonic sandstone (70 and 77; Condie, 1993). These observations suggest mild to moderate chemical weathering conditions in the source area. However, the range of CIA values clearly deviates from the ideal weathering trend parallel to A-CN line in the A-CN-K (Al_2O_3 – (CaO^* + Na_2O) – K_2O) diagram (Fig. 7a; Nesbitt et al., 1996), resulting from changing rates of chemical weathering and physical erosion over time, possibly as a consequence of tectonic instability in the source area.

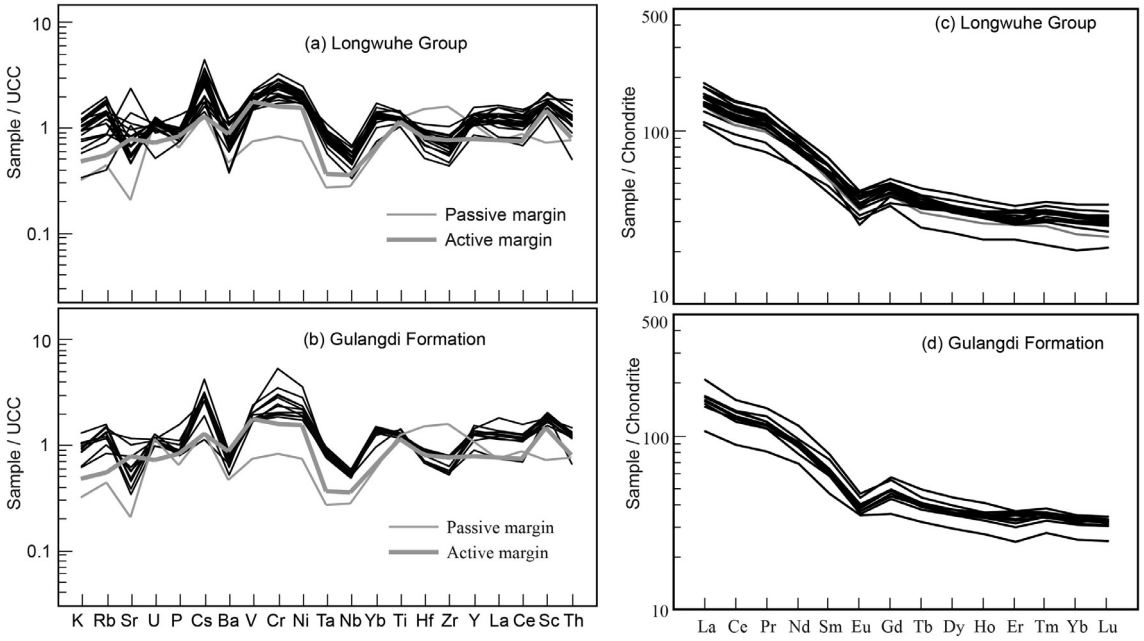

Fig. 5. UCC-normalized multi-element and chondrite-normalized REE plots of clastic rocks. Upper Continental Crust (UCC) and Chondrite normalized values are from Taylor and McLennan (1985).

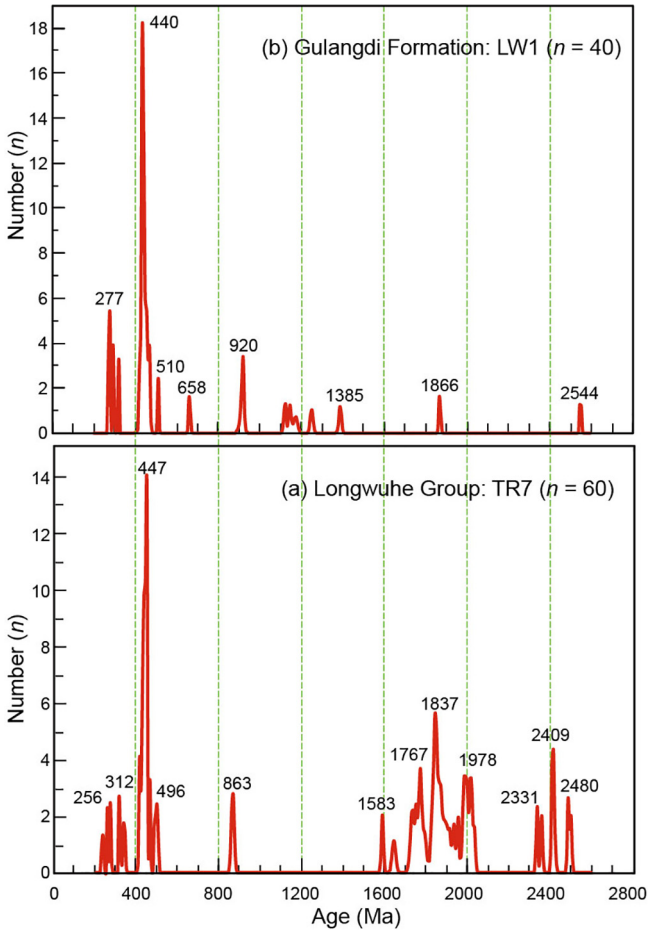

Fig. 6. Detrital zircon age probability histograms for Lower and Middle Triassic sandstone samples. Detrital zircon data with discordance equal to or less than 10%.

The Plagioclase Index of Alternation [PIA = 100 × (Al_2O_3 − K_2O)/(Al_2O_3 + CaO* + Na_2O − K_2O)] suggested by Fedo et al. (1995) is also used to estimate the degree of source weathering and elemental distribution during diagenesis. The analyzed samples have a variable range of PIA values (51–81) with an average of 61, which is higher than unweathered plagioclase (50) but less than the Post Archean Average Shale (PAAS; 79). This indicates abundant phyllosilicate mineralogy within the analyzed samples. In addition, the variable and high Th/U ratios (2.08–6.91; avg. 4.51) also demonstrate intense weathering in source areas or sediment recycling (McLennan et al., 1993). Together, CIA, PIA, and Th/U values demonstrate variable chemical weathering conditions in the source area that was likely closely related to tectonic instability.

6.2. Recycling and maturation

Among the major elements in clastic sediments, SiO_2 and Al_2O_3 reflect the content of quartz and clay minerals respectively, and the Fe_2O_3/K_2O ratio reflects mineralogical stability and distinguishes lithic fragments from feldspar. With an increasing SiO_2/Al_2O_3 ratio the grain size also increases, as does the extent of recycling and maturity of sediment. The average SiO_2/Al_2O_3 ratio (=3.3) for samples is similar to basic rocks (ca. 3) but less than evolved felsic rocks (ca. 5) (Roser et al., 1996), indicating low compositional maturity and correspondingly less sedimentary recycling. High K_2O/Na_2O ratio (1.32–3.41) is also indicative of chemical immaturity.

On the SiO_2/Al_2O_3 and Fe_2O_3/K_2O classification diagram of Herron (1988), most samples are classified as unstable immature wacke (Fig. 8a) with others as shale. According to the geochemical classification of Pettijohn et al. (1987), all samples, however, are greywacke (Fig. 8b), with high Na_2O/K_2O ratio and low Al_2O_3 and K_2O contents. Additionally, Al and Ti are usually considered to be stable during weathering and accumulate in the residue. On the Al_2O_3-TiO_2-Hf ternary diagram of Garcia et al. (1994), samples display a relative narrow range of TiO_2-Hf variation (Fig. 7b), suggesting poor sorting and compositional immaturity.

Recycling is closely related to transport and both can result in increasing CIW and CIA. Crustal materials from large source areas are usually transported for a long distance so that they have high CIW and

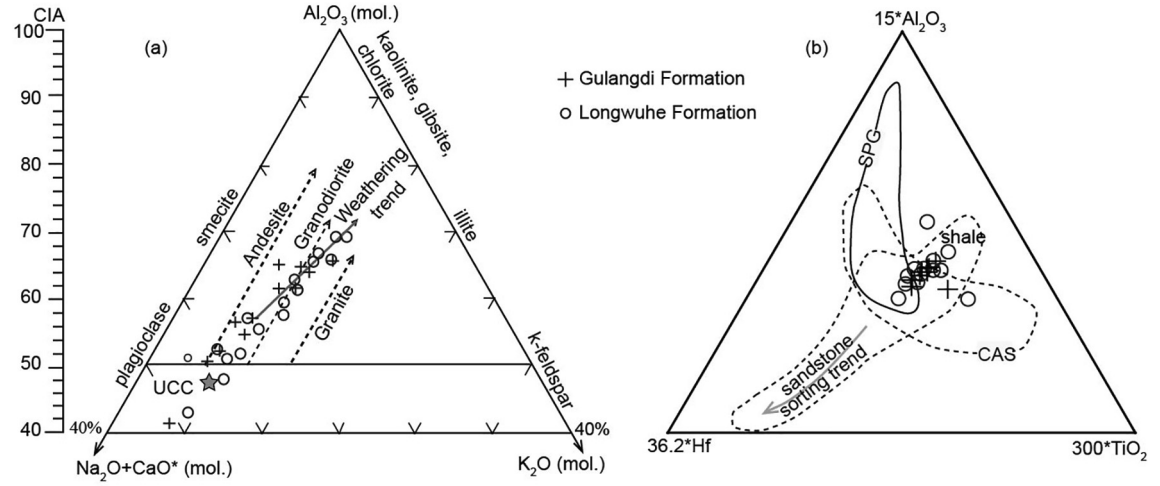

Fig. 7. (a) Al_2O_3 − CaO* + Na_2O − K_2O (A-CN-K) molecular proportion diagram (after Nesbitt and Young, 1982) for clastic rocks with Chemical Index of Alteration (CIA) scale. (b) Ternary plot of Al_2O_3*15 − 36.2*Hf − TiO_2*300 diagram (after Garcia et al., 1994). CAS, field of calc-alkaline granites; SPG, field of strongly peraluminous granites.

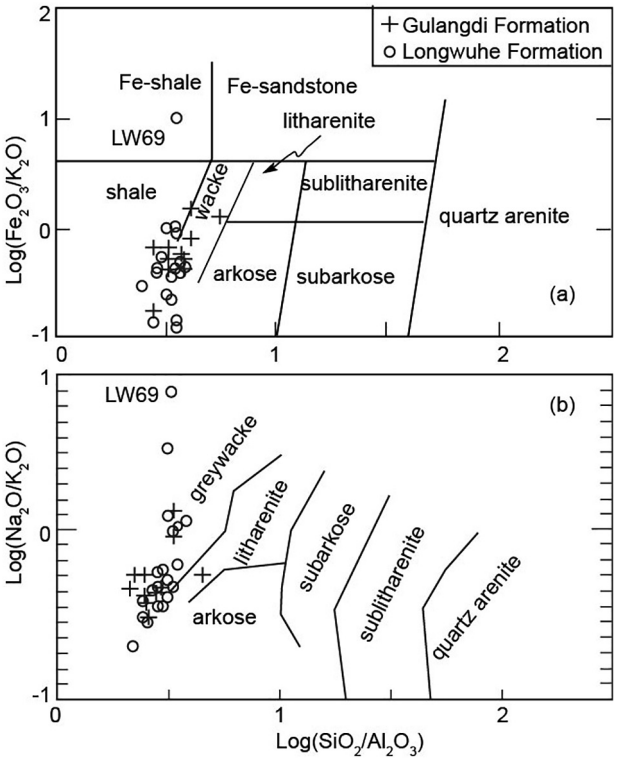

Fig. 8. Chemical classification scheme for Triassic siliciclastic rocks of the West Qinling Mountains. (a) Na_2O/K_2O-SiO_2/Al_2O_3 (after Pettijohn et al., 1987). (b) Fe_2O_3/K_2O-SiO_2/Al_2O_3 (after Herron, 1988).

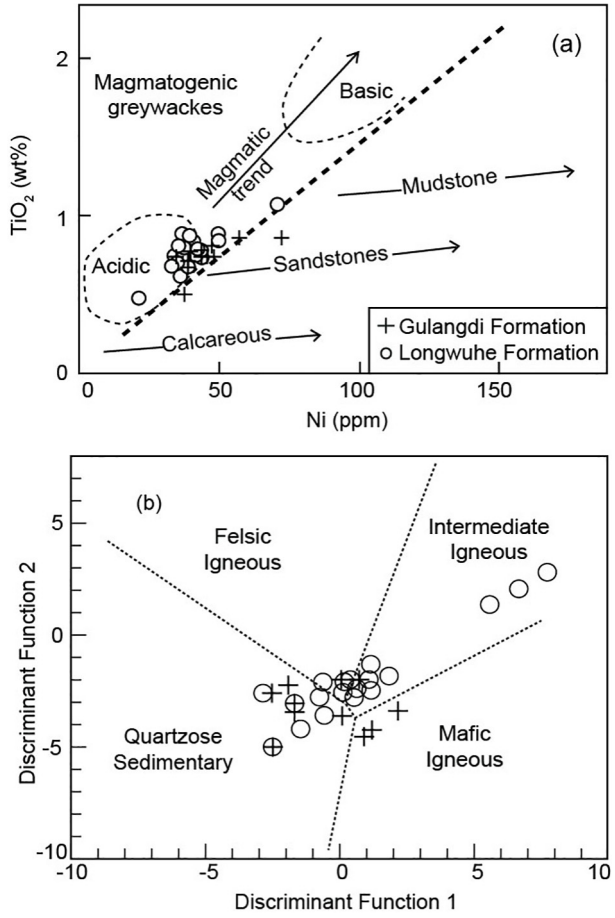

Fig. 9. (a) TiO_2-Ni plot of the siliciclatic rocks (Floyd et al., 1989), showing that all samples follow a typical magmatic trend for intermediate and felsic rocks. (b) Discriminant function diagram for the provenance signatures of clastic rocks using major elements (after Roser and Korsch, 1988).

CIA values (Gao et al., 1999). However, juvenile crustal materials from local sources are characterized by low CIW and CIA values because of little or no transport. The average CIW value (=73) amongst the present samples is greater than felsic gneiss (ca. 60; Gao et al., 1999), apparently indicating that the detritus from broad catchment area underwent long distance transportation before final deposition.

In order to further assess the issue of recycling, we use the relatively immobile elements Ti and Ni to discriminate between primary and sedimentary reworking controls on sediment compositions based on the discrimination plot of Floyd et al. (1989). On the TiO_2-Ni diagram, all samples fall within the compositional fields of immature sediments controlled by magmatic precursor rocks (Fig. 9a). This result implies that detritus was likely deposited very near its source with little recycling, which is also supported by low Zr concentrations (avg. 156 ppm). The apparent contradiction between these two assessments can be resolved if the source rocks are distinct from typical felsic gneiss. For example, the value of 73 is similar to the fresh pyroxene andesite

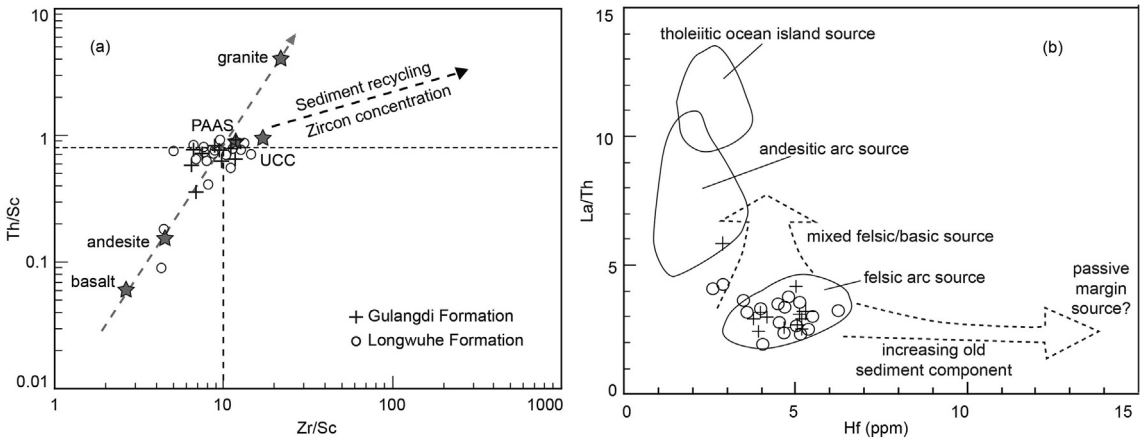

Fig. 10. (a) Th/Sc versus Zr/Sc (McLennan et al., 1993). (b) La/Th versus Hf discrimination diagrams illustrating weathering and sediment recycling (after Floyd and Leveridge, 1987). PAAS and UCC values are from Taylor and McLennan (1985).

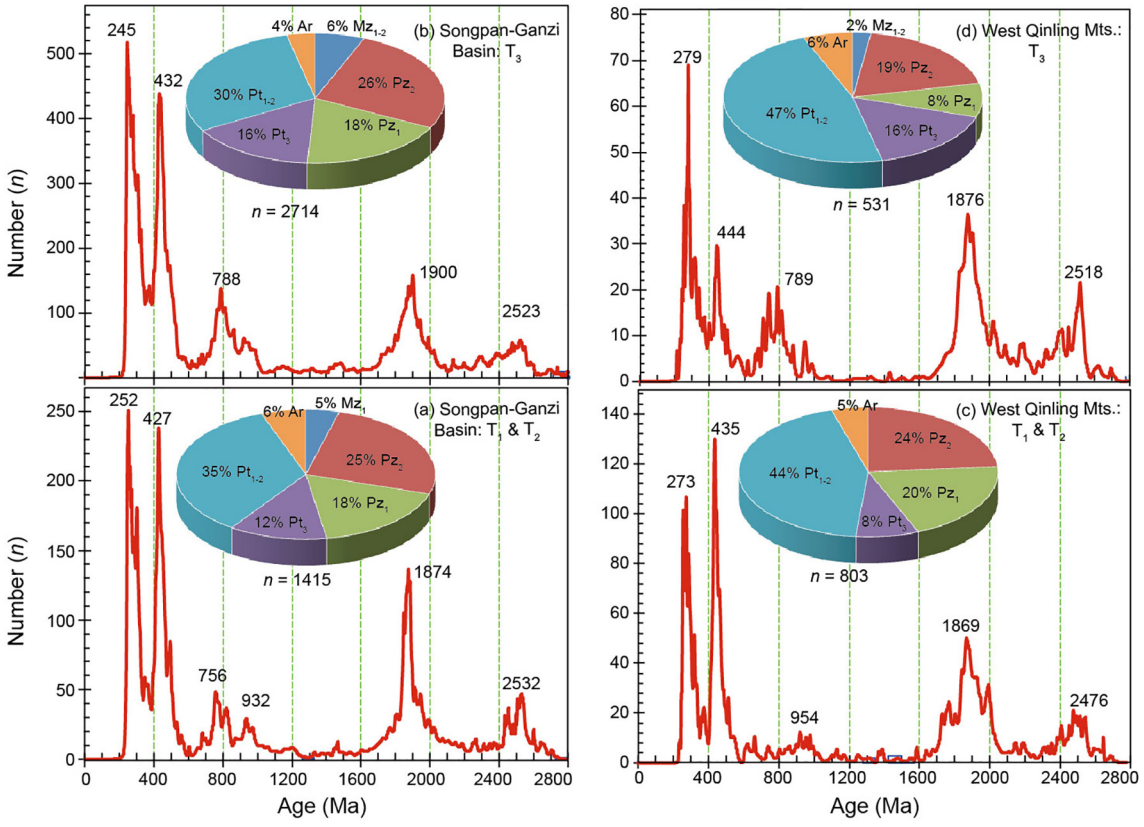

Fig. 11. Detrital zircon U-Pb age probability histograms of the Triassic siliciclastic samples in the Sonpan-Ganzi Basin and West Qinling Mountains. Data is after from Weislogel et al. (2010), Ding et al. (2013), Tang et al. (2018), Jian et al. (2019), and this study.

(ca. 66; X.W. Li et al., 2013) and lower than unweathered potassic granite (80; Fedo et al., 1995), which suggests that the detritus only underwent short distance transportation before final deposition.

In another way, the degree of recycling, heavy mineral sorting, and compositional variation can be assessed by using the Th/Sc-Zr/Sc (McLennan et al., 1990, 1993) and La/Th-Hf (Floyd and Leveridge, 1987) discriminant diagrams. A positive linear correlation between the Th/Sc and Zr/Sc ratios expresses first-cycle sediments, whereas additionally recycled sediments usually show a more rapid Zr/Sc than Th/Sc increase (Fig. 10a). Samples mainly follow the magmatic compositional variation trend, with slight displacement towards higher Zr/Sc ratios (> 10), suggestive of minor sediment reworking and sorting. These processes may also be reflected in the La/Th-Hf diagram (Fig. 10b; Floyd and Leveridge, 1987), in which sediment recycling in the Longwuhe Group and Gulangdi Formation appears to be less significant.

7. Provenance and tectonic setting of Lower to Middle Triassic sediments

7.1. Provenance

Al_2O_3/TiO_2 ratios of Lower to Middle Triassic sediments (18–25) in this study are similar to intermediate-felsic igneous rocks (19–28; Girty et al., 1996), and their REE patterns are also comparable to felsic igneous rocks showing high La_N/Yb_N ratios and negative Eu anomalies

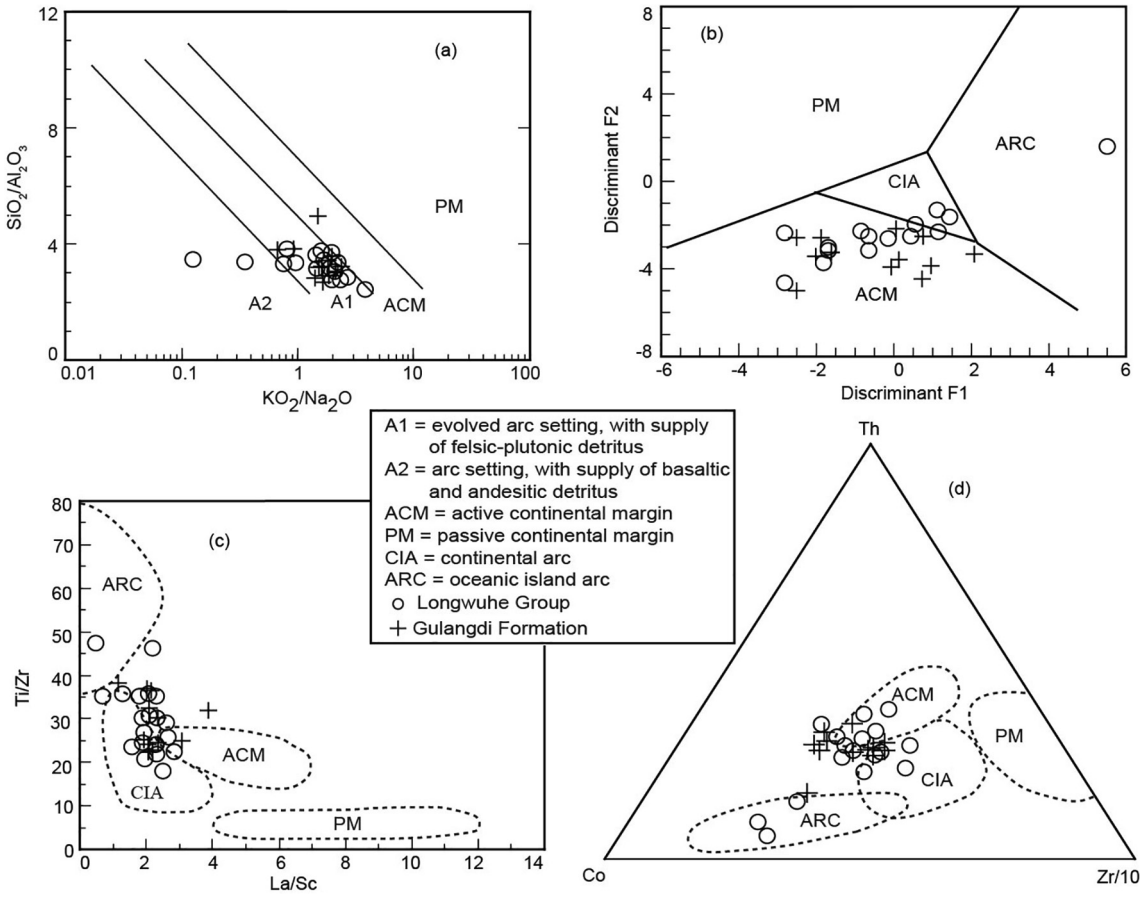

Fig. 12. Tectonic setting discriminant diagram of Longwuhe Group and Gulangdi Formation clastic rocks. (a) SiO_2/Al_2O_3 versus K_2O/Na_2O diagram after Roser and Korsch (1986); (b) discriminant function plot of Bhatia (1983); (c) Ti/Zr versus La/Sc and (d) Th-Co-Zr/10 diagrams after Bhatia and Crook (1986).

(Rollinson, 1993). On the discrimination plot of Floyd et al. (1989) (Fig. 9a), almost all samples plot in the magmatogenic greywacke field associated with felsic to intermediate igneous sources.

Generally, basic volcanic or plutonic detritus is enriched in Sc and Ti in comparison with more felsic material. Th/Sc and Zr/Sc ratios increase with sediment maturation and/or with the supply of felsic detritus, whereas Ti/Zr decreases. Lower Th/Sc (0.09–0.74) and higher Ti/Zr (17.7–48.18) values compared to the UCC (0.75 and 18.55, respectively) demonstrate that Triassic sediments in the West Qinling Mountains were primarily derived from felsic rocks. On the Th/Sc-Zr/Sc plot (Fig. 10a), most samples clustering close to the UCC and PAAS follow the compositional variation trend of magmatic rocks and are mainly distributed between andesite and granite compositions.

On the other hand, Triassic sediments plot in the fields of intermediate and felsic igneous rocks and recycling of older sedimentary rocks on the provenance discrimination diagram of Roser and Korsch (1988) (Fig. 9b). This indicates direct derivation of primary magmatic sources with some older sedimentary source rocks and/or gneisses, which contain polycyclic quartzose detritus. This inference is constant to the petrological and heavy mineral results (Yan et al., 2014).

In order to discriminate between the detailed sources of Triassic sediments of the West Qinling Mountains and Songpan-Ganzi Basin, published detrital zircon U-Pb age data (Weislogel, 2008; Weislogel et al., 2010; Ding et al., 2013; Tang et al., 2018; Jian et al., 2019) are combined together with new data from this study to develop age probability histograms. Detrital zircon age distributions for Triassic siliciclastic samples in the West Qinling Mountains and Songpan-Ganzi Basin are similar (Fig. 11), but the relative abundances of grains within age populations suggest that they originated from different source rocks. Paleoproterozoic and minor Archean and Neoproterozoic grains occur in all samples, but Paleozoic zircon grains show distinct abundance patterns within various age populations. The Paleozoic grains of the Lower- and Middle-Triassic sediments in the West Qinling Mountains mainly include Early Permian (ca. 273 Ma) and Early Silurian (ca. 435 Ma), whereas these in the Songpan-Ganzi Basin are dominated by ca. 252 Ma and ca. 427 Ma. The Upper-Triassic sediments of the West Qinling Mountains contain a much lesser proportion of Paleozoic detrital zircon grains (including ca. 279 Ma and ca. 444 Ma) than those of the Songpan-Ganzi Basin (ca. 432 Ma). The latter also contains some Middle Triassic (ca. 245 Ma) grains.

Paleocurrent analysis results (Zhou and Graham, 1996; Weislogel et al., 2010; Ding et al., 2013; L. Li et al., 2014; Jian et al., 2019) indicate that Triassic sediments in the West Qinling Mountains were mostly derived from a source to the north, whereas the associated sediments in the Songpan-Ganzi Basin was dominated by a mixed source to the northeastward and westward. Together, these results demonstrate that Triassic sediments in the West Qinling Mountains were primarily derived from the South Qilian Belt, comprising voluminous Ordovician to Silurian granitoids and Precambrian metamorphosed igneous and sedimentary rocks. Paleoproterozoic (peak at ~1.84 Ga) and Neoarchean (peak at ~2.5 Ga) grains were like derived from the North China Block basement, and Neoproterozoic grains (950–786 Ma) originated from the South Qilian Belt and East Kunlun basement. However, the Carboniferous-Permian volcano-magmatic complex (Kou et al., 2007) and ophiolite mélange (Guo et al., 2007) in the middle and NW of study area also represent another potential source.

7.2. Tectonic setting

Although the geochemistry of sediments is generally affected by

Table 1
Trace-element ratios of siliciclastic rocks used for discrimination of tectonic setting for the Longwuhe Group and Gulangdi Formation.

Provenance type	Sc/Cr	La/Sc	Th/Sc	La/Y	La/Th	La/Yb	La_N/Yb_N	Th/U	Ti/Zr	Eu/Eu*	ΣREE	Tectonic setting
Undissected magmatic arc	0.57 ± 0.16	0.55 ± 0.22	0.15 ± 0.08	0.48 ± 0.12	4.26 ± 1.20	4.2 ± 1.30	2.8 ± 0.90	2.1 ± 0.78	56.8 ± 21.4	1.04 ± 0.11	58 ± 10	ARC[#]
Dissected magmatic arc	0.32 ± 0.06	1.82 ± 0.30	0.85 ± 0.13	1.02 ± 0.07	2.36 ± 0.30	11 ± 40	7.5 ± 2.50	4.6 ± 0.45	19.7 ± 4.30	0.79 ± 0.13	146 ± 20	CIA [#]
Uplifted basement	0.30 ± 0.02	4.55 ± 0.80	2.95 ± 0.50	1.33 ± 0.09	1.77 ± 0.10	12.50	8.50	4.8 ± 0.38	15.3 ± 2.40	0.60	186	ACM [#]
Craton interior tectonic highlands	0.16 ± 0.02	6.25 ± 1.35	3.06 ± 0.80	1.31 ± 0.26	2.22 ± 0.47	15.90	10.80	5.6 ± 0.37	6.74 ± 0.90	0.56	210	PM[#]
Gulangdi Formation	0.21 ± 0.05	2.24 ± 0.62	0.70 ± 0.12	1.26 ± 0.31	3.24 ± 0.88	12.31 ± 2.29	8.31 ± 155	4.41 ± 0.82	28.99 ± 5.71	0.30 ± 0.28	198 ± 56	ACM/CIA
Longwuhe Group	0.23 ± 0.13	1.96 ± 0.58	0.66 ± 0.21	1.3 ± 0.33	3.07 ± 0.61	12.12 ± 3.08	8.17 ± 2.07	4.56 ± 0.97	30.04 ± 7.69	0.34 ± 0.31	165 ± 42	ACM/CIA

ARC = oceanic island arc; CIA = continental arc; ACM = active continental margin; PM = passive continental margin.
[#] Data from Bhatia and Crook (1986) and Bhatia (1985).

sorting, heavy mineral contents, and the proportion of mafic input, some geochemical discriminant diagrams or criteria have been successfully used to infer the tectonic setting of ancient sedimentary basins (e.g., Floyd et al., 1991; Japsen et al., 2007; Ryan and Williams, 2007; Yan et al., 2012; Pe-Piper et al., 2016; Higgs and King, 2018). In these diagrams, sediments are grouped into three or four categories based on their geochemical signal: oceanic island arc (ARC), continental arc (CIA), active continental margin (ACM), and passive continental margin (PM).

According to K_2O/Na_2O-SiO_2/Al_2O_3 and major-element oxides discriminant diagrams, the Lower to Middle Triassic sediments in the West Qinling Mountains were deposited in an ACM setting (Fig. 12). On the Ti/Zr-La/Sc and Th-Co-Zr/10 discriminant diagrams (Bhatia and Crook, 1986), samples plot in and around CIA and ACM fields with some in the ARC field. In addition, trace element distribution patterns for these sediments are similar to those of an ACM setting with distinct Nb-Ta and Zr-Hf troughs (Rollinson, 1993). These results favor deposition in ACM or CIA environments.

Sediments from PM to ACM through CIA to ARC show systematic increases in Sc/Cr, Ti/Zr, V/La and La/Th ratios and decreases in La_N/Yb_N, Th/U, La/Y, La/Sc, and Th/Sc ratios. Europium anomalies also decrease from PM to ARC. Based on comparisons of sediments from different tectonic setting (Bhatia, 1985; Bhatia and Crook, 1986), these parameters indicate that Triassic sediments are nearly identical to those deposited in ACM or CIA settings (Table 1). Distinctive negative Eu anomalies, LREE-enriched patterns, and weak fractionation of HREE also support this finding. Generally, CIA and ACM are similar depositional environments as both are dominated by convergent plate motions, orogenic deformation, the development of subduction complexes, and are underlain by continental crust.

Multi-element diagrams normalized to UCC provide a complimentary approach to bivariate plots to assess the tectonic setting of clastic sediments, although they are strongly influenced by heavy mineral contents, mafic input, and the degree of sorting (Floyd et al., 1991). On the multi-element diagram, the studied samples display rather strong enrichment in Cs and V-Cr-Ni-Ti-Sc, and a generalized depletion in Nb-Ta and Zr-Hf. The pronounced negative Sr anomaly and enrichment in Y is typical for old recycled environments and passive continental margin settings (Floyd et al., 1989). However, the positive V-Cr-Ni-Ti-Cs anomalies and strong Nb-Ta depletions of the entire sample are indicative of an active margin or continental arc setting. The presence of these two types of signatures is common in active margins in which sedimentation is characterized by a mixture of young arc-derived material of variable composition and old upper crustal material (McLennan et al., 1990, 1993; Yan et al., 2012). It indicates that some old sedimentary detritus from the arc-basement was added to the sediments because of strong uplift and erosion during Early to Middle Triassic time.

7.3. Tectonic affinity

Together geochemical and petrological data point to an intermediate to felsic igneous rock source within an active continental margin for Lower to Middle Triassic deposits in the West Qinling Mountains. This interpretation is also supported by the geochemistry of detrital Cr-spinel, pyroxene, and amphiboles (Yan et al., 2014).

Regionally, widespread Early to Middle Triassic Andean-type volcanism and magmatism occurred in the West Qinling Mountains and extended westward into the Kunlun Mountains (Xiao et al., 2002; Qiang et al., 2007; Guo et al., 2012; Yan et al., 2012; Dong et al., 2012, 2017; Niu et al., 2018). A EW-trending continental arc developed side along the south of the Qilian Orogen and was superposed onto the Early- and Late-Paleozoic ophiolite mélanges in the West Qinling Mountains and South Qilian-Kunlun belt. Voluminous detritus from this belt was transported southward until it was blocked by the A'nimaqen-Mianlue ophiolitic mélange. Sediments were deposited in a forearc basin

between the arc and the ophiolitic mélange but were not transported to the south into the Songpan-Ganzi Basin.

8. Conclusions

(1) Lower to Middle Triassic turbidites in the West Qinling Mountains mainly consist of feldspathic litharenite and lithic arkose with low mineral and compositional maturity.
(2) Detrital sediments originated from a primary continental arc source dominated by intermediate to felsic igneous rocks, with a minor contribution from older metamorphosed and sedimentary sources.
(3) Detrital zircon dating indicates that Early- and Middle-Triassic turbidites of the West Qinling Mountains are dominated by detritus eroded from sourcs with ca. 273 Ma, 435 Ma and 1869 Ma ages and are thus different from those in the Songpan-Ganzi Basin.
(4) These sediments were deposited in a forearc basin that developed above a northward subducting slab of the Paleo-Tethyan ocean lithosphere.

Declaration of Competing Interest

The authors declare that they have no known competing financial interests or personal relationships that could have appeared to influence the work reported in this paper.

Acknowledgements

Professor Shu Sun is a prestigious sedimentologist, who made important contributions to Geoscience. We would like to commemorate Mr. Sun Shu with this article. Support for this work was provided by the National Natural Science Foundation of China (Grants 41872241, 41672221, and 41702239) and China Geological Survey (Grants DD20190006, DD20160201-04). We greatly appreciate constructive and helpful reviews by Professor Sanzhong Li, an anonymous reviewer and comments by Editor Professor Mei-Fu Zhou that considerably improved this manuscript.

Appendix A. Supplementary material

Supplementary data to this article can be found online at https://doi.org/10.1016/j.jaesx.2019.100020.

References

Basu, A., Young, S.W., Suttner, L.J., James, W.C., Mack, G.H., 1975. Reevaluation of the use of undulatory extinction and polycrystallinity in detrital quartz for provenance interpretation. J. Sediment. Petrol. 45, 873–882.
Dickinson, W.R., Gehrels, G.E., 2009. U-Pb ages of detrital zircons in Jurassic eolian and associated sandstones of the Colorado Plateau: evidence for transcontinental dispersal and intraregional recycling of sediment. Geol. Soc. Am. Bull. 121, 408–433.
BGMRGP (Bureau of Geology and Mineral Resources of Gansu Province), 1989. Regional Geology of Gansu Province. Geological Memoir 19. Geological Publishing House, Beijing, pp. 692.
BGMRQP (Bureau of Geology and Mineral Resources of Qinghai Province), 1991. Regional Geology of Qinghai Province. Geological Memoir 21. Geological Publishing House, Beijing, pp. 664.
Bhatia, M.R., 1983. Plate tectonics and geochemical composition of sandstones. J. Geol. 91, 611–627.
Bhatia, M.R., 1985. Rare earth element geochemistry of Australian Paleozoic graywackes and mud rocks: provenance and tectonic control. Sed. Geol. 45, 97–113.
Bhatia, M.R., Crook, K.A.W., 1986. Trace element characteristics of graywackes and tectonic setting of sedimentary basins. Contrib. Miner. Petrol. 92, 181–193.
Bian, Q., Li, D., Pospelov, I.I., Yin, L., Li, H., Zhao, D., Chang, C., Luo, X., Gao, S., Aatrakhantsev, O., Chamov, N., 2004. Age, geochemistry, and tectonic setting of Buqingshan ophiolites, North Qinghai-Tibet Plateau, China. J. Asian Earth Sci. 23, 577–596.
Brugier, O., Lancelot, J.R., Malavieille, J., 1997. U-Pb dating on single zircon grains from the Triassic Songpan-Garze flysch (Central China): provenance and tectonic correlations. Earth Planet. Sci. Lett. 152, 217–231.
Chang, E.Z., 2000. Geology and tectonics of the Songpan-Ganzi fold belt, southwestern China. Int. Geol. Rev. 42, 813–831.
Chen, B., Wang, K., Liu, W., Cai, Z., Zhang, Q., Peng, X., Qiu, Y., Zheng, Y., 1987. Geotectonics of the Nujiang-Lancangjiang-Jinshajiang Region. Geological Publishing House, Beijing, pp. 204.
Condie, K.C., 1993. Chemical composition and evolution of the upper continental crust: contrasting results from surface samples and shales. Chem. Geol. 104, 1–37.
Dickinson, W.R., Gehrels, G.E., 2008. Sedimentary delivery to the Cordilleran foreland basin: Insights from U-Pb ages of detrital zircons in Upper Jurassic and Cretaceous strata of the Colorado Plateau. Am. J. Sci. 308, 1041–1082.
Ding, L., Yang, D., Cai, F.L., Pullen, A., Kappa, P., Gehrels, G.E., Zhang, L.Y., Zhang, Q.H., Lai, Q.Z., Yue, Y.H., Shi, R.D., 2013. Provenance analysis of the Mesozoic Hoh-Xil-Songpan-Ganzi turbidites in northern Tibet: Implications for the tectonic evolution of the eastern Paleo-Tethys Ocean. Tectonics 32, 34–48.
Dong, Y., He, D., Sun, S., Liu, X., Zhou, X., Zhang, F., Yang, Z., Cheng, B., Zhao, G., Li, J., 2017. Subduction and accretionary tectonics of the East Kunlun Orogen, western segment of the Central China Orogenic System. Earth Sci. Rev. https://doi.org/10.1016/j.earscirev.2017.12.006.
Dong, Y.P., Liu, X.M., Zhang, G.W., Chen, Q., Zhang, X.N., Li, W., Yang, C., 2012. Triassic diorites and granitoids in the Foping area: constraints on the conversion from subduction to collision in the Qinling orogen, China. J. Asian Earth Sci. 47, 123–142.
Enkelmann, E., Weislogel, A., Ratschbacher, L., Eide, E., Renno, A., Wooden, J., 2007. How was the Triassic Songpan-Ganzi basin filled? A provenance study. Tectonics 26, TC4007. https://doi.org/10.1029/2006TC002078.
Fedo, C.M., Nesbitt, H.M., Young, G.M., 1995. Unraveling the effects of potassium metasomatism in sedimentary rocks and paleosols, with implications for paleoweathering conditions and provenance. Geology 23, 921–924.
Feng, Y., Cao, X., Zhang, E., 2002. Orogenic Belt of the Western Qinling. Xi'an Cartography Publishing House, Xi'an, pp. 263.
Floyd, P.A., Leveridge, B.E., 1987. Tectonic environments of Devonian Gramscatho basin, south Cornwall: framework mode and geochemical evidence from turbiditic sandstones. J. Geol. Soc. 144, 181–204.
Floyd, P.A., Shail, R., Leveridge, B.E., Franke, W., 1991. Geochemistry and provenance of Rhenohercynian synorogenic sandstones: implications for the tectonic environment discrimination. Geol. Soc. Spec. Pub. 57, 173–188.
Floyd, P.A., Winchester, J.A., Park, R.G., 1989. Geochemistry and tectonic setting of Lewisian clastic metasediments from the Early Proterozoic Loch Maree Group of Gairloch, NW Scotland. Precambr. Res. 45, 203–214.
Gao, S., Ling, W.L., Qiu, Y.M., Lian, Z., Hartmann, G., Simon, K., 1999. Contrasting geochemical and Sm-Nd isotopic compositions of Archean metasediments from the Kongling high-grade terrain of the Yangtze craton: evidence for cratonic evolution and redistribution of REE during crustal anatexis. Geochim. Cosmochim. Acta 63, 2071–2088.
Garcia, D., Fonteilles, M., Moutte, J., 1994. Sedimentary fractionations between Al, Ti, and Zr and the genesis of strongly peraluminous granites. J. Geol. 102, 411–422.
Girty, G.H., Ridge, D.L., Knaack, C., Johnson, D., Al-Riyami, R.K., 1996. Provenance and depositional setting of Paleozoic chert and argillite, Sierra Nevada, California. J. Sediment. Res. 66, 107–118.
Gehrels, George, Valencia, Victor, Pullen, Alex, 2006. Detrital Zircon Geochronology by Laser-Ablation Multicollector ICPMS at the Arizona LaserChron Center. Paleontol. Soc. pap. 12, 67–76. https://www.cambridge.org/core/product/identifier/S1089332600001352/type/journal_articlehttps://doi.org/10.1017/S1089332600001352.
Gu, X.X., 1994. Geochemical characteristics of the Triassic Tethys turbidites in northwestern Sichuan, China: implications for provenance and interpretation of the tectonic setting. Geochim. Cosmochim. Acta 58, 4615–4631.
Guo, A., Zhang, G., Sun, Y., Zheng, J., Liu, Y., Wang, J., 2007. Geochemistry and spatial distribution of OIB and MORB in A'nyemaqen ophiolite zone: evidence of Majixueshan ancient ridge-centered hotspot. Sci. China Ser. D - Earth Sci. 50, 197–208.
Guo, X., Yan, Z., Wang, Z., Wang, T., Hou, K., Fu, C., Li, J., 2012. Middle-Triassic arc magmatism along the northeastern margin of the Tibet: U-Pb and Lu-Hf zircon characterization of the Gangcha complex in the West Qinling terrane, central China. J. Geol. Soc. 169, 327–336.
Harnois, L., 1988. The CIW index: a new chemical index of weathering. Sed. Geol. 55, 319–322.
Herron, M.M., 1988. Geochemical classification of terrigenous sands and shales from core or log data. J. Sediment. Petrol. 58, 820–829.
Higgs, K.E., King, P.R., 2018. Sandstone provenance and sediment dispersal in a complex tectonic setting: Taranaki Basin, New Zealand. Sed. Geol. 372, 112–139.
Jackson, S.E., Pearson, N.J., Griffin, W.L., Belousova, E.A., 2004. The application of laser ablation-inductively coupled plasma-mass spectrometry to in situ U-Pb zircon geochronology. Chem. Geol. 211, 47–69.
Japsen, P., Green, P.F., Nielsen, L.H., Rasmussen, E.S., Bidstrup, T., 2007. Mesozoic-Cenozoic exhumation events in the eastern North Sea Basin: a multi-disciplinary study based on palaeothermal, palaeoburial, stratigraphic and seismic data. Basin Res. 19, 451–490.
Jian, X., Weislogel, A., Pullen, A., 2019. Triassic sedimentary filling and closure of the eastern Paleo-Tethys Ocean: New insights from detrital zircon geochronology of Songpan-Ganzi, Yidun, and West Qinling flysch in eastern Tibet. Tectonics 38, 767–787.
Jiang, X., Pan, G., Yan, Y., Li, Z., 1996. Triassic sedimentary framework and tecto-paleogeographic evolution of the junction of the Qinling, Qilian and Kunlun orogenic belts. Acta Geologica Sichuan 16, 204–208.
Klimetz, M.P., 1983. Speculations on the Mesozoic plate tectonic evolution of eastern China. Tectonics 2, 139–166.
Kou, X., Zhu, Y., Zhang, K., Shi, B., Luo, G., 2007. Discovery and geochemistry of upper Permian volcanic rocks in Tongren area, Qinghai province and their tectonic significance. J. China Univ. Geosci. 32, 45–50.

Lai, S., Wang, G., Li, S., 2004. Ophiolites from the Mianlue suture in the southern Qinling and their relationship with the eastern Paleotethys evolution. Acta Geol. Sin. 78, 107–117.

Li, R.B., Pei, X.Z., Li, Z.C., Pei, L., Chen, Y.X., Liu, C.J., Chen, G.C., Liu, T.J., 2015. The depositional sequence and prototype basin for Lower Triassic Hongshuichuan Formation in the eastern segment of East Kunlun Mountains. Geol. Bull. China 34, 2302–2314.

Li, S.Z., Jahn, B.M., Zhao, S.J., Dai, L.M., Li, X.Y., Suo, Y.H., Guo, L.L., Wang, Y.M., Liu, X.C., Lan, H.Y., Zhou, Z.Z., Zheng, Q.L., Wang, P.C., 2017. Triassic southeastward subduction of North China Block to South China Block: Insights from new geological, geophysical and geochemical data. Earth Sci. Rev. 166, 270–285.

Li, S.Z., Zhao, S.J., Liu, X., Cao, H.H., Yu, S., Li, X.Y., Somerville, I., Yu, S.Y., Suo, Y.H., 2018. Closure of the Proto-Tethys Ocean and Early Paleozoic amalgamation of microcontinental blocks in East Asia. Earth Sci. Rev. 186, 37–75.

Li, X.W., Mo, X.X., Yu, X.H., Ding, Y., Huang, X.F., Wei, P., He, W.Y., 2013. Petrology and geochemistry of the early Mesozoic pyroxene andesites in the Maixiu Area, West Qinling, China: products of subduction or syn-collision? Lithos 172–173, 158–174.

Li, L., Meng, Q., Pullen, A., Garzione, C.N., Wu, G., Wang, Y., Ma, S., Duan, L., 2014a. Late Permian-early Middle Triassic back-arc basin development in West Qinling, China. J. Asian Earth Sci. 87, 116–129.

Li, X.W., Mo, X.X., Bader, T., Scheltens, M., Yu, X.H., Dong, G.A., Huang, X.F., 2014b. Petrology, geochemistry and geochronology of the magmatic suite from the Jianzha Complex, central China: petrogenesis and geodynamic implications. J. Asian Earth Sci. 95, 164–181.

Ludwig, K.R., 2003. Isoplot 3.0: A geochronological toolkit for Microsoft Excel, vol. 4, 1–70.

McLennan, S.M., Hemming, S., McDaniel, D.K., Hanson, G.N., 1993. Geochemical approaches to sedimentation, provenance and tectonics. Geol. Soc. Am. Spec. Pap. 284, 21–40.

McLennan, S.M., Taylor, S.R., McCulloch, M.T., Maynard, J.B., 1990. Geochemical and Nd-Sr isotopic composition of deep-sea turbidites: crustal evolution and plate tectonic associations. Geochim. Cosmochim. Acta 54, 2015–2050.

Meng, Q.R., Zhang, G.W., 1999. Timing of collision of the North and South China blocks: Controversy and reconciliation. Geology 27, 123–126.

Nesbitt, H.W., Young, G.M., 1982. Early Proterozoic climates and plate motions inferred from major elements chemistry of lutites. Nature 299, 715–717.

Nesbitt, H.W., Young, G.M., McLennan, S.M., Keays, R.R., 1996. Effects of chemical weathering and sorting on the petrogenesis of siliciclastic sediments, with implications for provenance studies. J. Geol. 104, 525–542.

Nie, S., Yin, A., Rowley, D.B., Jin, Y., 1994. Exhumation of the Dabie Shan ultrahigh-pressure rocks and accumulation of the Songpan-Ganzi flysch sequence, central China. Geology 22, 999–1002.

Niu, M.L., Zhao, Q.Q., Wu, Q., Li, X.C., Yan, Z., Li, J.L., Sun, Y., Yuan, X.Y., 2018. Magma mixing identified in the Guokeshan pluton, northern margin of the Qaidam basin: evidence from petrology, mineral chemistry, and whole-rock geochemistry. Acta Petrol. Sin. 34, 1991–2016.

Olivarius, M., Rasmussen, E.S., Siersma, V., Knudsen, C., Kokfelt, T.F., Keulen, N., 2014. Provenance signal variations caused by facies and tectonics: zircon age and heavy mineral evidence from Miocene sand in the north-eastern North Sea Basin. Mar. Pet. Geol. 49, 1–14.

Pe-Piper, G., Piper, D.J.W., Ying, W., Zhang, Y., Trottier, C., Ge, C., Yin, Y., 2016. Quaternary evolution of the rivers of northeast Hainan Island, China: tracking the history of avulsion from mineralogy and geochemistry of river and delta sands. Sed. Geol. 333, 84–99.

Pettijohn, F.J., Potter, P.E., Siever, R., 1987. Sand and Sandstone, second ed. Springer-Verlag, Berlin, pp. 553.

Pullen, A., Kapp, P., Gehrels, G.E., Vervort, J.D., Ding, L., 2008. Triassic continental subduction in central Tibet and Mediterranean-style closure of the Paleo-Tethys Ocean. Geology 36, 5351–5354.

Qiang, J., Guo, A., Sun, Y., 2007. Geochemistry of granitoids of the Zongwulongshan tectonic zone and geological significance. J. Northwest Univ. 37, 98–102.

Rollinson, H.R., 1993. Using Geochemical Data: Evaluation, Presentation, Interpretation. Longman Scientific and Technical London, pp. 352.

Roser, B., Korsch, R., 1986. Determination of tectonic setting of sandstone-mudstone suites using SiO_2 content and K_2O/Na_2O ratio. J. Geol. 94, 635–650.

Roser, B.P., Cooper, R.A., Nathan, S., Tulloch, A.J., 1996. Reconnaissance sandstone geochemistry, provenance and tectonic setting of lower Paleozoic terranes of the West Coast and Nelson, New Zealand. N. Z. J. Geol. Geophys. 39, 1–16.

Roser, B.P., Korsch, R.J., 1988. Provenance signatures of sandstone–mudstone suites determined using discriminant function analysis of major-element data. Chem. Geol. 67, 119–139.

Rudnick, R.L., Gao, S., 2003. The Composition of the Continental Crust. In: Rudnick, R.L. (Ed.), The Crust. Elsevier-Pergamon, Oxford, pp. 1–64.

Ryan, K.M., Williams, D.M., 2007. Testing the reliability of discrimination diagrams for determining the tectonic depositional environment of ancient sedimentary basins. Sed. Geol. 5, 54–56.

Sengör, A.M.C., Altiner, D., Cin, A., Ustaömer, T., Hsü, K.J., 1988. Origin and assembly of the Tethyside orogenic collage at the expense of Gondwana-land. Geol. Soc. Spec. Pub. 37, 119–181.

She, Z., Ma, C., Masona, R., Li, J., Wang, G., Lei, Y., 2006. Provenance of the Triassic Songpan-Ganzi flysch, west China. Chem. Geol. 231, 159–175.

Stampfli, G.M., Borel, G.D., 2002. A plate tectonic model for the Paleozoic and Mesozoic. Earth Planet. Sci. Lett. 196, 17–33.

Sun, Y., Zhang, G., Wang, J., Zhan, F., Zhang, Z., 2004. $^{40}Ar/^{39}Ar$ age of the basic swarms of two periods in the junction area of Qinling and Kunlun and its tectonic significance. Acta Geol. Sin. 78, 65–71.

Sun, J., Xiao, W., Windley, B.F., Ji, W., Fu, B., Wang, J., Jin, C., 2016. Provenance change of sediment input in the northeastern foreland of Pamir related to collision of the Indian Plate with the Kohistan-Ladakh arc at around 47Ma. Tectonics 35, 315–338.

Tang, Y., Zhang, Y., Tong, L., 2018. Mesozoic-Cenozoic evolution of the Zoige depression in the Songpan-Ganzi flysch basin, eastern Tibetan Plateau: constraints from detrital zircon U-Pb ages and fission-track ages of the Triassic sedimentary sequence. J. Asian Earth Sci. 151, 285–300.

Taylor, S.R., McLennan, S.M., 1985. The Continental Crust: Its Composition and Evolution. Blackwell Scientific Publishers, Oxford, pp. 312.

Wang, B., Zhang, Z., Zhang, S., Zhu, Y., Cao, S., 2000. Geological features of lower Paleozoic ophiolite in Kuhai-Saishitang region, eastern section of Eastern Kunlun. Journal of China University of Geosciences 25, 592–598.

Weislogel, A.L., 2008. Tectonostratigraphic and geochronologic constraints on evolution of the northeast Paleotethys from the Songpan-Ganzi complex, central China. Tectonophysics 451, 331–345.

Weislogel, A.L., Graham, S.A., Chang, E.Z., Wooden, J.L., Gehrels, G.E., Yang, H.S., 2006. Detrital zircon provenance of the Late Triassic Songpan-Ganzi complex: sedimentary record of collision of the North and South China blocks. Geology 34, 97–100.

Weislogel, A.L., Graham, S.A., Chang, E.Z., Wooden, J.L., Gehrels, G.E., 2010. Tectonics, erosional exhumation, and sediment production Upper Triassic Songpan-Ganzi complex, central China: record of collisional detrital zircon provenance from three turbidite depocenters. Geol. Soc. Am. Bull. 122, 2041–2062.

Xiao, W.J., WindLey, B.F., Chen, H.L., Zhang, G.C., Li, J.L., 2002. Carboniferous-Triassic subduction and accretion in the western Kunlun, China: implications for the collisional and accretionary tectonics of the northern Tibetan Plateau. Geology 30, 295–298.

Xie, X.L., Niu, M.L., Wu, Q., Yan, Z., Li, X.C., Xia, W.J., Fu, C.L., 2015. Petrological characteristics of Triassic magmatic rocks from conjunction of Qinling, Qilian, and Kunlun Orogens and their tectonic environment. J. Earth Sci. Environ. 37, 72–81.

Xu, Z.Q., Yang, J.S., Chen, F.Y., 1996. The A'nyemaqen suture belt and the dynamicas in subduction and collision. In: Zhang, Q. (Ed.), Study on Ophiolites and Geodynamics. Geological Publishing House, Beijing, pp. 185–189.

Yan, Z., Bian, Q.T., Korchagin, O.A., Pospelov, I.I., Li, J.L., Wang, Z.Q., 2008. Provenance of early Triassic Hongshuichuan Formation in the southern margin of the East Kunlun Mountains: Constrain from detrital framework, heavy mineral analysis and geochemistry. Acta Petrol. Sin. 24, 1068–1078.

Yan, Z., Guo, X., Fu, C., Aitchison, J.C., Li, J., 2014. Detrital heavy mineral constraints on the Triassic tectonic evolution of the West Qinling Terrane, NW China: implications for understanding subduction of the Paleotethyan Ocean. J. Geol. 122, 591–608.

Yan, Z., Wang, Z., Yan, Q., Wang, T., Guo, X., 2012. Geochemical constraints on the provenance and depositional setting of the Devonian Liuling Group, East Qinling Mountains, central China: implications for the tectonic evolution of the Qinling orogenic belt. J. Sediment. Res. 82, 9–20.

Yang, J., Wang, X., Shi, R., Xu, Z., Wu, C., 2004. The Dur'ngoi ophiolite in East Kunlun, northern Qinghai-Tibet Plateau: a fragment of Paleo-Tethyan oceanic crust. Chin. Geol. 31, 225–239.

Zhou, D., Graham, S.A., 1996. Songpan-Ganzi Triassic flysch complex of the West Qinling Shan as a remnant ocean basin. In: Yin, A., Harrison, M. (Eds.), The Tectonic Evolution of Asia. Cambridge University Press, Cambridge, pp. 281–299.